

## Correlation-Driven Charge and Spin Fluctuations in $\text{LaCoO}_3$

M. Karolak,<sup>1</sup> M. Izquierdo,<sup>2,3,4</sup> S. L. Molodtsov,<sup>2,5,6</sup> and A. I. Lichtenstein<sup>2,3</sup>

<sup>1</sup>*Institut für Theoretische Physik und Astrophysik, Universität Würzburg, Am Hubland, 97074 Würzburg, Germany*

<sup>2</sup>*European XFEL GmbH, Albert-Einstein-Ring 19, 22761 Hamburg, Germany*

<sup>3</sup>*I. Institut für Theoretische Physik, Universität Hamburg, Jungiusstraße 9, 20355 Hamburg, Germany*

<sup>4</sup>*Synchrotron Soleil, L'Orme des Merisiers St-Aubin, BP-48, 91192 Gif-sur-Yvette, France*

<sup>5</sup>*Institute of Experimental Physics, Technische Universität Bergakademie Freiberg, 09599 Freiberg, Germany*

<sup>6</sup>*ITMO University, Kronverkskiy prospekt 49, 197101 St. Petersburg, Russia*

(Received 14 January 2015; revised manuscript received 27 April 2015; published 21 July 2015)

The spin transition in  $\text{LaCoO}_3$  has been investigated using density-functional theory in combination with dynamical mean-field theory employing continuous time quantum Monte Carlo and exact diagonalization impurity solvers. Calculations on the experimental rhombohedral atomic structure with two Co sites per unit cell show that an independent treatment of the Co atoms results in a ground state with strong charge fluctuations induced by electronic correlations. Each atom shows a contribution from either a  $d^5$  or a  $d^7$  state in addition to the main  $d^6$  state. These states play a relevant role in the spin transition which can be understood as a low spin-high spin (LS-HS) transition with significant contributions ( $\sim 10\%$ ) to the LS and HS states of  $d^5$  and  $d^7$  states, respectively. We report spectra as well as optical conductivity data for all cases. A thermodynamic analysis reveals a significant kinetic energy gain through introduction of charge fluctuations, which in addition to the potential energy reduction lowers the total energy of the system.

DOI: 10.1103/PhysRevLett.115.046401

PACS numbers: 71.27.+a, 71.10.Fd, 71.15.Mb, 71.30.+h

The rich physics of  $\text{LaCoO}_3$  (LCO), especially the nonmagnetic to magnetic transition has been an intriguing research topic for decades (see, e.g., Ref. [1]). The debate regarding the origin of the transition and its understanding in terms of the spin states of the  $\text{Co}^{3+}$  ion is ongoing. The competing models are the low-spin (LS,  $t_{2g}^6 e_g^0$ ) to high spin (HS,  $t_{2g}^4 e_g^2$ ) mechanism [2] and the low-spin to intermediate spin (IS,  $t_{2g}^5 e_g^1$ ) model with concomitant orbital ordering [3]. The interest in this system has been recently boosted by the potential applications of this material and its doped phases in various environmental-friendly energy production domains [4]. From the theoretical point, LCO addresses one of the most challenging problems beyond band theory approaches: the treatment of strongly correlated materials with well-formed paramagnetic local moments. Although the addition of static local correlations to density functional theory (DFT +  $U$ ) [5] improved the description of correlated materials with long range magnetic order, only the more advanced formalism combining DFT with dynamical mean-field theory (DMFT) [6] describes paramagnetic systems with local moments satisfactorily [7]. The development and extension of this methodology is also of importance for understanding the properties of other classes of materials like colossal magnetoresistance in manganites [8], or high temperature superconductors [9].

Many-body calculations on LCO have been performed within DFT + DMFT [10] and the variational cluster approximation (VCA) [11]. In the first case, the spin state transition was described as a smooth crossover from the homogeneous LS state into a nonhomogeneous mixture of

all three spin states. On the other hand, the VCA calculations showed that only the LS and HS states play a role [11]. The most recent attempts to settle the matter by means of DFT + DMFT [12,13] used continuous-time quantum Monte Carlo (CT-QMC) impurity solvers [14]. In both calculations, an LS-HS transition results. No evidence of an IS configuration was obtained, even upon going beyond the  $d^6$  ionic picture [13]. Including  $d^7$  and  $d^8$  states to describe the local dynamics of the system allows us to interpret the spin state transition as an LS (with few HS ions) to an LS-HS short range ordered phase, with a subsequent melting of the order at higher temperatures. At room temperature, when 50% LS-HS population is expected, a Co(LS)-O-Co (HS) arrangement is anticipated. Most of the many-body calculations assumed equivalent Co atoms, except for a couple of DFT +  $U$  works [15,16]. In a ground-breaking study on a two band Hubbard model, Kuneš and Křápek [17] showed that charge imbalance between sites can occur on purely electronic grounds and possibly constitutes an important piece in the LCO spin state transition puzzle.

In this Letter, we bolster this proposal by reporting on the first *ab initio* study of correlation-driven charge and spin fluctuations in LCO within the DFT + DMFT formalism for inequivalent Co atoms. Our results show that symmetry breaking of the Co sites creates a correlation-driven charge and spin fluctuation of purely electronic origin.  $\text{LaCoO}_3$  is a perovskite showing a small tetragonal distortion of the  $\text{CoO}_6$  octahedra that varies with temperature [18]. To describe it, we start from DFT calculations using the experimentally determined structures for 5 K, 300 K, and

650 K. We use a rhombohedral unit cell containing two formula units. The VASP code [19] with projector augmented wave basis sets [20,21] and the Perdew-Burke-Ernzerhof [22] functional was employed. A Wannier type construction using projected local orbitals, as described in [23,24], was applied to construct a low energy model, which contains the on-site energies and hoppings extracted from DFT. We focus here on the 3d orbitals of Co, avoiding ambiguities that arise from the use of  $d + p$  models in DFT + DMFT [25,26]. Since the system is not cubic, a straightforward Wannier construction produces a basis that retains on-site mixing between the Co  $t_{2g}$  and  $e_g$  orbitals. This local  $t_{2g}$ - $e_g$  hybridization is mostly a consequence of the choice of orbital representation; therefore, we have performed a unitary transformation to minimize it. The usual choices are a rotation into the so-called “crystal field basis” or into a basis that locally diagonalizes the DFT occupancy matrix [27,28]. The data presented were obtained using the latter approach. We have explored both approaches and found that the choice has no qualitative effect.

In DFT, we find a set of three orbitals very close in energy (two  $e_g^\pi$  and one  $a_{1g}$ , that we, for brevity, call  $t_{2g}$ ) and two orbitals ( $e_g$ ) higher in energy by about  $\Delta \sim 1.5$ – $1.65$  eV. We solve an effective multiorbital Hubbard model within DMFT using hybridization expansion CT-QMC [14,29] as well as exact diagonalization (ED, Lanczos method [30]) as solvers. To treat the two Co atoms in the unit cell independently, we employ the so-called inhomogeneous or real space DMFT [31], where we have to solve an impurity model for each correlated atom  $\alpha$  in the unit cell, and the atoms effectively interact via their respective baths of conduction electrons. The effective five band model including the Coulomb interaction and a double counting correction (DC), then, contains the following terms:

$$\hat{H} = \hat{H}^0 - \sum_{\alpha, m, \sigma} \mu_{\alpha}^{\text{DC}} \hat{n}_{\alpha m, \sigma} + \frac{1}{2} \sum_{\alpha, i, j} U_{\alpha}^{ijkl} \hat{c}_{\alpha i \sigma}^{\dagger} \hat{c}_{\alpha j \sigma'}^{\dagger} \hat{c}_{\alpha l \sigma'} \hat{c}_{\alpha k \sigma},$$

where  $\hat{H}^0$  is the DFT Hamiltonian,  $\hat{c}_{\alpha i \sigma}^{\dagger}$  is the creation operator of an electron on site  $\alpha$  in Wannier state  $i$  and spin  $\sigma$ . The double counting,  $\propto \mu_{\alpha}^{\text{DC}}$ , amounts to a shift of the chemical potential for the Co 3d shell and is determined self consistently [32]. To obtain the Coulomb interaction matrix, we employ the parametrization via Slater integrals [38] connected to the average direct and exchange couplings  $U$  and  $J$ :  $F^0 = U$ ,  $J = 1/14(F^2 + F^4)$  and  $F^4 = 0.625F^2$ . Depending on the solver, either the full Coulomb interaction (ED) or terms proportional to  $\hat{n}_{\alpha i, \sigma} = \hat{c}_{\alpha i \sigma}^{\dagger} \hat{c}_{\alpha i \sigma}$  (QMC) were used.

To properly describe the system within DFT + DMFT the appropriate choice of the Coulomb interaction is crucial. In the case of LCO, the problem is delicate since after the DFT +  $U$  calculations that introduced the LS-IS model [3], it has been widely believed that it is strongly

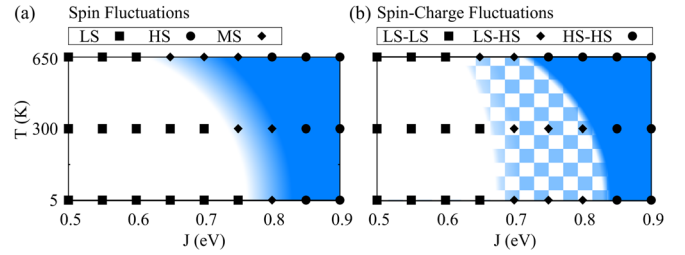


FIG. 1 (color online). Phase diagram as a function of the lattice temperature and the Hunds rule coupling  $J$  for  $U = 3$  eV. The colored (shaded) parts illustrate different regions, white indicating LS and blue (gray) HS. (a) Homogeneous phase exhibiting the LS, MS, and HS states as indicated by the data points. (b) shows the data points and possible phase regions for the calculation with inequivalent Co atoms. The checkerboard pattern now indicating the LS-HS phase where strong charge fluctuations are present.

correlated with an on-site Coulomb interaction of  $U = 8$  eV. Recently, constrained DFT results proposed a value of  $U = 6$  eV [13]. Such values might be appropriate in  $d + p$  models, but are, however, too large for  $d$  only calculations. Since we are not aware of any *ab initio* estimates for the Co 3d shell only, measurements of the excitation gap in LCO have been used as a guide. A gap of about 0.9 eV was measured from photoemission and absorption spectra [39], while 0.6 eV [40] and 0.3 eV [41] were obtained from optical measurements. We were able to obtain a charge gap  $\sim 1$  eV with a value of  $U = 3$  eV, which was used in all subsequent calculations. We have, however, explored the effects of increasing the Coulomb interaction [32].

Since the value of the Hunds coupling  $J$  is, for a fixed  $U$  and crystal field splitting  $\Delta$ , the critical parameter for the spin transition [42] we have calculated the system at different values of  $J$ . To account for the temperature, the calculations were performed for the experimental lattice structures determined at the temperatures 5 K, 300 K and 650 K [18]. In the impurity solver we used the calculation temperatures 116 K, 290 K, 580 K (inverse temperatures  $\beta = 100, 40, 20$  eV $^{-1}$ ) for these structures respectively.

In a first approximation, the two Co atoms were constrained to be in the same charge and spin state. The calculations show that for the three crystal structures and their respective crystal fields a spin state transition occurs at about  $\Delta \sim 2J$ , i.e., for  $J \sim 0.75$ – $0.8$  eV. In Fig. 1a we have plotted our data for  $U = 3$  eV as a function of the “lattice temperature” and  $J$ . We can see that there is a crossover region, that we call mixed spin (MS), between the homogeneous LS (white region) and HS (blue region) phases. The transition is governed by an increased admixture of the HS contribution to the LS state. The CT-QMC solver allows for an analysis of the local eigenstates contributing to the partition function during the imaginary time evolution. The states observed here are almost pure LS or HS ( $> 90\%$  probability), i.e.,  $d_{S=0}^6$  and  $d_{S=2}^6$  with

no contributions from IS ( $d_{S=1}^6$ ) and small ( $\sim 3\%$ ) ones from  $d_{S=1/2}^5$  and  $d_{S=3/2}^7$ .

In a second step, the constraint of equivalent Co atoms was removed. In this way, we can take the first step beyond single-site DMFT and explore how susceptible the system is to charge fluctuations between neighboring Co atoms. The calculations show that within this assumption, strong charge fluctuations between the two ions develop. This can happen spontaneously via noise introduced by the QMC procedure without introducing a double-counting correction (or with identical double countings on both atoms), but we have also introduced a small difference in the levels ( $\mu_1^{\text{DC}} - \mu_2^{\text{DC}} = 0.02$  eV) in the first DMFT iteration to render the two atoms explicitly inequivalent [43]. This is akin to a “kick” often used to explicitly break a symmetry of the system, e.g., in magnetic calculations. At small  $J$ , the two atoms both converge to the LS configuration as before, but with increasing  $J$  charge fluctuations between the two atoms occur, see the LS-HS region in Fig. 1(b).

Regarding the spin configuration, in the LS-HS phase, one atom will be in a predominantly LS and the other in a predominantly HS state. Additionally, the occupancies of the Co 3d shells deviate from  $N_{3d} = 6$ , see Table I. Consequently, the QMC partition function shows sizeable contributions of  $d_{S=1/2}^7$  on atom 1 and  $d_{S=3/2}^5$  on atom 2, respectively. Other theoretical results and the interpretation of experiments [2,44] indicate that such a state exists in LCO at room temperature. The charge disproportionation observed here is expected to improve the quantitative agreement with experimental data as already realized in Ref. [13]. Moreover, the presence of  $d^5$  and  $d^7$  states will produce new terms in the soft x-ray absorption spectra that are expected to contribute significantly at the low energy side of the Co- $L_3$  edge, where  $d^6$  cluster calculations result in too low intensity [44].

To clarify, since the Co atoms are equivalent by lattice symmetry, in an exact solution of the correlated model for LCO, a static charge disproportionation would not be present. Charge ordering has been seen in thin films of LCO, but there is no evidence of it in the bulk [45]. Nevertheless, nonlocal dynamical charge fluctuations should

be very strong in bulk LCO due to the proximity to the surface (thin film) charge-density-wave instability. In a hypothetical exact calculation, these effects would be encoded in the frequency dependence of the nonlocal electronic self-energy  $\Sigma(\mathbf{k}, \omega)$ . Since  $\Sigma(\mathbf{k}, \omega)$  cannot be calculated for such a complex multiorbital system, we model charge fluctuations in the local DMFT theory using the possibility of a broken symmetry solution between the Co atoms. The tendency of the DMFT to establish charge order in the parameter range relevant for the spin state transition gives an indication of possible charge fluctuations in bulk LCO. However, DMFT is known to overestimate ordering tendencies and, in certain cases, even predict order, where there should be none, like in the two dimensional Hubbard model [46].

From Fig. 1, one can see that the spin transition can be studied as a function of the Hunds coupling  $J$  and of the temperature. This implies, that the transition can be driven only by electronic means, as shown by model calculations [17]. In the following, electronic structure will be investigated as a function of  $J$  assuming the 300 K crystal structure, which exhibits all relevant features. The evolution of the Co 3d spectra as a function of  $J$  is given in Fig. 2. The orbitally resolved spectral function (obtained via maximum entropy [47] from the QMC Green’s function) is shown for the homogeneous LS and HS states of the 300 K crystal structure in Fig. 2(a). Changes occur especially in the unoccupied part of the spectra, suggesting

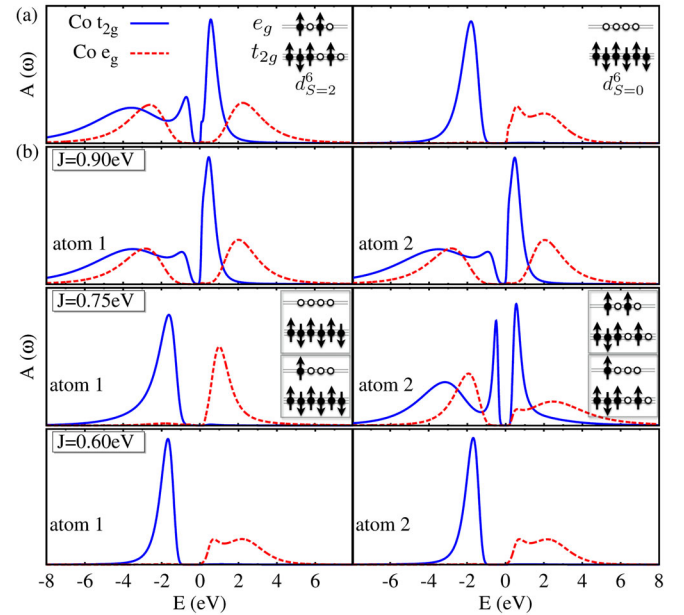


TABLE I. Most probable many-body configurations for the 300 K structure with two inequivalent Co atoms as a function of the Hunds coupling  $J$  obtained from the analysis of the CT-QMC imaginary time evolution (in %). Numbers missing to 100% are due to minor contributions of other atomic states.

$J$ (eV)	Co ( $N_{3d}$ )	$d_{S=0}^6$	$d_{S=1/2}^5$	$d_{S=1/2}^7$	$d_{S=3/2}^5$	$d_{S=3/2}^7$	$d_{S=2}^6$
0.60	1 (6.0)	93	4	3	...	...	...
	2 (6.0)	93	4	3	...	...	...
0.75	1 (6.1)	81	3	15	...	...	...
	2 (5.9)	...	...	...	12	3	82
0.90	1 (6.0)	...	...	...	3	7	87
	2 (6.0)	...	...	...	3	7	87

FIG. 2 (color online). Orbitally resolved spectral functions for the 300 K crystal structure at solver temperature of 290 K. (a) The homogeneous HS ( $J = 0.9$  eV, left) and LS spectra ( $J = 0.6$  eV, right) with atomic states given as an inset. (b) Results for the asymmetric Co configuration for the values of  $J$  indicated along with the largest and second largest many-body contributions in the LS-HS phase.



that experiments addressing those states will be relevant to understanding the system in more detail [48]. The LS state in Fig. 2(a) is closest to the DFT solution, the strongest modification is the rigid upward shift of the  $e_g$  bands and, as a consequence, the gap opening between the  $t_{2g}$  and  $e_g$  states. This is in accordance with combined DFT and cluster calculations [49] as well as recent DFT + DMFT [13]. The formation of local moments in the higher temperature HS states leads to the appearance of additional features in the spectrum. As a result, the gap changes its character from  $t_{2g}$ - $e_g$  to  $t_{2g}$ - $t_{2g}$  with incoherent  $t_{2g}$  excitations on both gap edges. The occupied parts of the spectra exhibit a transfer of spectral weight away from the strong  $t_{2g}$  excitation peak towards higher binding energies as the LS to HS crossover commences [13]. The spectral function for the asymmetric Co configuration is displayed in Fig. 2(b) for the LS-LS ( $J = 0.6$  eV), the LS-HS ( $J = 0.75$  eV), and the HS-HS ( $J = 0.9$  eV) arrangements. Again, as the transition from LS-LS to HS-HS commences via LS-HS, the weight of the  $t_{2g}$  excitation peak is increasingly redistributed. Also, the progressive reduction of the gap expected from experiments is observed [44,49,50]. The tendency of the system to introduce charge fluctuations can be understood by analyzing the total energies for all relevant situations. Considering the one-electron, kinetic and potential energies, one finds a region where the LS-HS state is energetically favored [32].

For the 300 K structure, we have also performed ED calculations using five sites to parametrize the bath (5 + 5 model) and the full Coulomb interaction. The spectra obtained using this methodology are shown in Figs. 3(a) and 3(b) and are qualitatively close to the QMC spectra; differences are understood as inherent methodological ones. Since ED gives us immediate access to real frequency quantities, we were able to calculate the optical conductivity, as shown in Fig. 3(c) using the approach of Ref. [51]. Details concerning this calculation are given in the Supplemental Material [32]. Since only the Co  $d$  bands were included, only  $d$ - $d$  transitions are captured and  $d$ - $p$  or other transitions are neglected. Comparing to the DFT result, which has a Drude contribution at the Fermi level and a secondary peak at  $\sim 0.5$  eV, we see that all solutions show semiconducting behavior with a “foot” followed by the onset of interband transitions. The data show a clear trend: the LS has the largest gap with a gradual increase of the response beyond 2 eV, while the HS phase has a smaller gap followed by a peak. The LS-HS state is at low energy following the HS, but with a weaker feature around 1.5 eV and a more distinct feature around 2.5 eV. Experiments also find two main features, one at 1.5 eV that increases when the temperature is increased, marking the population of the HS state, as well as a second feature at 2.5 to 3.0 eV [52,53]. Thus, our data reproduce this general trend. However, it can only give a first hint at what to expect in an experiment. Especially, the onset of  $d$ - $p$  transitions can become important at energies higher than a few eV [51].

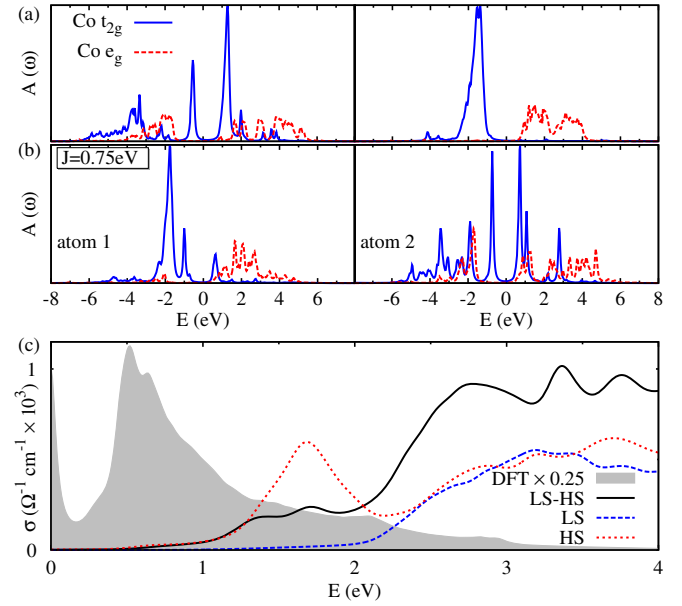


FIG. 3 (color online). Orbitaly resolved spectral functions for the 300 K crystal structure at solver temperature of 290 K obtained with ED. (a) The homogeneous HS ( $J = 0.9$  eV, left) and LS spectra ( $J = 0.6$  eV, right). (b) Results for the asymmetric Co configuration for  $J = 0.75$  eV. (c) Optical conductivity obtained using the ED self-energies as well as the Peierls approximation.

In summary, DFT + DMFT calculations for the two atomic unit cell of  $\text{LaCoO}_3$  show that, upon treating the Co atoms independently, strong charge fluctuations develop in the system. As a consequence, the spin transition can be understood as a transition from a homogeneous LS to a LS-HS state with strong charge fluctuations and, subsequently, into a homogeneous HS state. This provides a novel understanding of the system in which the charge fluctuations are present in the system from first principles. Angle resolved photoemission experiments as a function of the temperature and time-resolved x-ray absorption studies with femtosecond resolution should allow us to verify the proposed model.

The authors thank G. Sangiovanni and M. Veit for fruitful discussions. M. I. acknowledges BMBF Proposal No. 05K12GU2 for financial support. Financial support by the Deutsche Forschungsgemeinschaft (DFG) through SFB 668 and SFB 1170 (“ToCoTronics”) is gratefully acknowledged.

- [1] N. B. Ivanova, S. G. Ovchinnikov, M. M. Korshunov, I. M. Eremin, and N. V. Kazak, *Usp. Fiz. Nauk* **179**, 837 (2009) [*Phys. Usp.* **52**, 789 (2009)].
- [2] R. Heikes, R. Miller, and R. Mazelsky, *Physica (Utrecht)* **30**, 1600 (1964); P. M. Raccach and J. B. Goodenough, *Phys. Rev.* **155**, 932 (1967).
- [3] M. A. Korotin, S. Y. Ezhov, I. V. Solovyev, V. I. Anisimov, D. I. Khomskii, and G. A. Sawatzky, *Phys. Rev. B* **54**, 5309 (1996).

- [4] N. Li, A. Boréave, J.-P. Deloume, and F. Gaillard, *Solid State Ionics* **179**, 1396 (2008); M. Alifanti, J. Kirchnerova, B. Delmon, and D. Klvana, *Appl. Catal., A* **262**, 167 (2004); C. H. Kim, G. Qi, K. Dahlberg, and W. Li, *Science* **327**, 1624 (2010); O. Büchler, J. Serra, W. Meulenberg, D. Sebold, and H. Buchkremer, *Solid State Ionics* **178**, 91 (2007); M. C. Álvarez-Galván, D. A. Constantinou, R. M. Navarro, J. A. Villoria, J. L. G. Fierro, and A. M. Efstathiou, *Appl. Catal., B* **102**, 291 (2011).
- [5] V. I. Anisimov, F. Aryasetiawan, and A. I. Lichtenstein, *J. Phys. Condens. Matter* **9**, 767 (1997).
- [6] A. Georges, G. Kotliar, W. Krauth, and M. J. Rozenberg, *Rev. Mod. Phys.* **68**, 13 (1996).
- [7] G. Kotliar, S. Y. Savrasov, K. Haule, V. S. Oudovenko, O. Parcollet, and C. A. Marianetti, *Rev. Mod. Phys.* **78**, 865 (2006).
- [8] M. B. Salamon and M. Jaime, *Rev. Mod. Phys.* **73**, 583 (2001); Y.-F. Yang and K. Held, *Phys. Rev. B* **82**, 195109 (2010).
- [9] C. Weber, K. Haule, and G. Kotliar, *Nat. Phys.* **6**, 574 (2010); T. Maier, M. Jarrell, T. Pruschke, and M. H. Hettler, *Rev. Mod. Phys.* **77**, 1027 (2005); T. Tohyama, *Jpn. J. Appl. Phys.* **51**, 010004 (2012).
- [10] L. Craco and E. Müller-Hartmann, *Phys. Rev. B* **77**, 045130 (2008).
- [11] R. Eder, *Phys. Rev. B* **81**, 035101 (2010).
- [12] G. Zhang, E. Gorelov, E. Koch, and E. Pavarini, *Phys. Rev. B* **86**, 184413 (2012).
- [13] V. Křápek, P. Novák, J. Kuneš, D. Novoselov, D. M. Korotin, and V. I. Anisimov, *Phys. Rev. B* **86**, 195104 (2012).
- [14] E. Gull, A. J. Millis, A. I. Lichtenstein, A. N. Rubtsov, M. Troyer, and P. Werner, *Rev. Mod. Phys.* **83**, 349 (2011).
- [15] K. Knížek, Z. Jiráček, J. Hejtmánek, and P. Novák, *J. Phys. Condens. Matter* **18**, 3285 (2006).
- [16] K. Knížek, Z. Jiráček, J. Hejtmánek, P. Novák, and W. Ku, *Phys. Rev. B* **79**, 014430 (2009).
- [17] J. Kuneš, and V. Křápek, *Phys. Rev. Lett.* **106**, 256401 (2011).
- [18] P. G. Radaelli and S.-W. Cheong, *Phys. Rev. B* **66**, 094408 (2002).
- [19] G. Kresse and J. Hafner, *J. Phys. Condens. Matter* **6**, 8245 (1994).
- [20] P. E. Blöchl, *Phys. Rev. B* **50**, 17953 (1994).
- [21] G. Kresse and D. Joubert, *Phys. Rev. B* **59**, 1758 (1999).
- [22] J. P. Perdew, K. Burke, and M. Ernzerhof, *Phys. Rev. Lett.* **77**, 3865 (1996).
- [23] B. Amadon, F. Lechermann, A. Georges, F. Jollet, T. O. Wehling, and A. I. Lichtenstein, *Phys. Rev. B* **77**, 205112 (2008).
- [24] M. Karolak, T. O. Wehling, F. Lechermann, and A. I. Lichtenstein, *J. Phys. Condens. Matter* **23**, 085601 (2011).
- [25] N. Parragh, G. Sangiovanni, P. Hansmann, S. Hummel, K. Held, and A. Toschi, *Phys. Rev. B* **88**, 195116 (2013).
- [26] M. Karolak, G. Ulm, T. Wehling, V. Mazurenko, A. Poteryaev, and A. Lichtenstein, *J. Electron Spectrosc. Relat. Phenom.* **181**, 11 (2010).
- [27] F. Lechermann, A. Georges, A. Poteryaev, S. Biermann, M. Posternak, A. Yamasaki, and O. K. Andersen, *Phys. Rev. B* **74**, 125120 (2006).
- [28] E. Pavarini, A. Yamasaki, J. Nuss, and O. K. Andersen, *New J. Phys.* **7**, 188 (2005).
- [29] L. Huang, Y. Wang, Z. Y. Meng, L. Du, P. Werner, and X. Dai, *Comput. Phys. Commun.* **195**, 140 (2015).
- [30] M. Capone, L. de' Medici, and A. Georges, *Phys. Rev. B* **76**, 245116 (2007).
- [31] M. Potthoff and W. Nolting, *Phys. Rev. B* **59**, 2549 (1999).
- [32] See Supplemental Material at <http://link.aps.org/supplemental/10.1103/PhysRevLett.115.046401> for a detailed description of the energy balance, the calculation of the optical properties using exact diagonalization, as well as a discussion of the influence of the Coulomb interaction and double-counting parameters on the results, which includes Refs. [33–37].
- [33] K. Held, A. K. McMahan, and R. T. Scalettar, *Phys. Rev. Lett.* **87**, 276404 (2001).
- [34] I. Leonov, A. I. Poteryaev, V. I. Anisimov, and D. Vollhardt, *Phys. Rev. Lett.* **106**, 106405 (2011).
- [35] A. Amaricci, N. Parragh, M. Capone, and G. Sangiovanni, *arXiv:1310.3043*.
- [36] M. T. Czyżyk and G. A. Sawatzky, *Phys. Rev. B* **49**, 14211 (1994).
- [37] J. M. Tomczak and S. Biermann, *Phys. Rev. B* **80**, 085117 (2009).
- [38] J. C. Slater, *Quantum Theory of Atomic Structure* (McGraw-Hill, New York, 1960), Vol 1.
- [39] M. Abbate, J. C. Fuggle, A. Fujimori, L. H. Tjeng, C. T. Chen, R. Potze, G. A. Sawatzky, H. Eisaki, and S. Uchida, *Phys. Rev. B* **47**, 16124 (1993).
- [40] A. Chainani, M. Mathew, and D. D. Sarma, *Phys. Rev. B* **46**, 9976 (1992).
- [41] T. Arima, Y. Tokura, and J. B. Torrance, *Phys. Rev. B* **48**, 17006 (1993).
- [42] Y. Tanabe and S. Sugano, *J. Phys. Soc. Jpn.* **9**, 766 (1954).
- [43] We want to note that a very large initial imbalance ( $\mu_1^{\text{DC}} - \mu_2^{\text{DC}} \sim 1$  eV) leads, at large enough values of  $J$ , to a stabilization of a  $d_{S=5/2}^5 - d_{S=3/2}^7$  order. See [32] for details.
- [44] M. W. Haverkort, Z. Hu, J. C. Cezar, T. Burnus, H. Hartmann, M. Reuther, C. Zobel, T. Lorenz, A. Tanaka, N. B. Brookes, H. H. Hsieh, H.-J. Lin, C. T. Chen, and L. H. Tjeng, *Phys. Rev. Lett.* **97**, 176405 (2006).
- [45] M. Merz, P. Nagel, C. Pinta, A. Samartsev, H. v. Löhneysen, M. Wissinger, S. Uebe, A. Assmann, D. Fuchs, and S. Schuppler, *Phys. Rev. B* **82**, 174416 (2010).
- [46] A. A. Katanin, A. Toschi, and K. Held, *Phys. Rev. B* **80**, 075104 (2009).
- [47] M. Jarrell and J. E. Gubernatis, *Phys. Rep.* **269**, 133 (1996).
- [48] M. Izquierdo, M. Karolak, C. Trabant, K. Holldack, A. Föhlisch, K. Kummer, D. Prabhakaran, A. T. Boothroyd, M. Spiwek, A. Belozero, A. Poteryaev, A. Lichtenstein, and S. L. Molodtsov, *Phys. Rev. B* **90**, 235128 (2014).
- [49] M. Abbate, R. Potze, G. A. Sawatzky, and A. Fujimori, *Phys. Rev. B* **49**, 7210 (1994).
- [50] Z. Hu, H. Wu, T. C. Koethe, S. N. Barilo, S. V. Shiryaev, G. L. Bychkov, C. Schüssler-Langeheine, T. Lorenz, A. Tanaka, H. H. Hsieh, H.-J. Lin, C. T. Chen, N. B. Brookes, S. Agrestini, Y. Y. Chin, M. Rotter, and L. H. Tjeng, *New J. Phys.* **14**, 123025 (2012).
- [51] P. Wissgott, J. Kuneš, A. Toschi, and K. Held, *Phys. Rev. B* **85**, 205133 (2012).
- [52] D. W. Jeong, W. S. Choi, S. Okamoto, J.-Y. Kim, K. W. Kim, S. J. Moon, D.-Y. Cho, H. N. Lee, and T. W. Noh, *Sci. Rep.* **4**, 6124 (2014).
- [53] J. C. Reul, Phd. Thesis, University of Cologne, 2013.